Synthesis of some Mannich Base, evaluating their Biological Activity, and Studying their Effect on DNA through Binding

Khattab OmarAzeez[1], Ibtihal Qahtan Abdalluh[1], Hala M.G. Al-Zahawi[2]
[1]Chemistry Department, College of Science, University of TiKrit, Iraq
[2]Chemistry Department, College of Science, University of Kirkuk, Iraq
Email: Khattabomer7@gmail.com

Abstract

This article is concerned with the preparation of indole derivatives, including compound (1) KI6, compound (21) KI4, compound (20), compound (8) KI2 and compound (24) KI1, where all these compounds were identified through infrared and proton NMR. I n this research, the study appeared different biological activity of these compounds against gram-positive, gram-negative bacteria and fungals was studied, in addition to studying the effect of these compounds on the polymer DNA.

Keywords: Mannich base, indole derivative, inhibition zone.

1. Introduction

The classical Mannich reaction, a three-component condensation between structurally diverse substrates (XeH) containing at least one active hydrogen atom, an aldehyde component (generally R1-CHO) and an amine reagent leads to a class of compounds generally known as Mannich bases (scheme 1) . For the reason that Mannich bases may be considered derivatives of the substrate obtained through substitution by an aminoalkyl moiety, Mannich reactions are also known as aminoalkylation reactions. In the particular instance when formaldehyde is employed as aldehyde component, the substrate is converted into the corresponding Mannich base through an aminomethylation process. Although primary amines and even ammonia (in the form of an ammonium salt) may be employed as amine reagents in aminomethylations or aminoalkylations, secondary aliphatic amines (R2NH) are the most commonly encountered as amine reagents in the Mannich reaction. As formaldehyde is used to a great extent as aldehyde component in the Mannich reaction, the structural diversity of Mannich bases stems primarily from the miscellaneous types of the substrates that can be subjected to aminomethylation, and secondarily from the variety of amine reagents that can be potentially employed in the Mannich reaction. Regardless of their structural diversity, the substrates should all have an activating functional group as a crucial structural feature that is required to render the substrate active in the Mannich reaction. The carbonyl function in ketones, the phenolic hydroxyl in phenols, the terminal carbonecarbon triple bond in alkynes, the heteroatom in heterocycles, or electronwithdrawing groups that substitute the carbon atom a to the carboxylate group in esters of aliphatic carboxylic acids are common examples of pairs of activating groups and corresponding substrates, but the list is far from being exhaustive [1, 2].

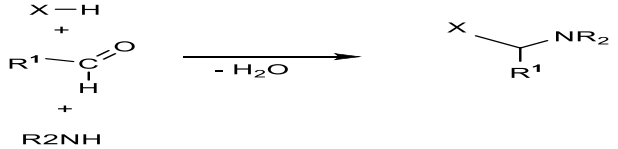

Scheme 1. General representation of the Mannich reaction.

Mannich reaction [3] is one of the most fundamental and important, C-C bond forming reactions in organic synthesis. Mannich reaction withstands a large diversity of functional groups and hence it has been witnessing a continuous growth in the field of Organic Chemistry. The flow of literature on Mannich reaction provides an outstanding evidence for the diversity and applications of the reaction [4-6]. The Mannich reaction and its variants offer a strong method for the preparation of the aminocarbonyl and several other derivatives [7]. The amino carbonyl Mannich products are useful in the construction of β- peptides and β-lactams, which are present in several bioactive molecules such as Tramadol, osnervan and moban are bioactive β-aminocarbonyl derivatives with analgesic, antiparkinson and neuroleptic properties taxol (antitumour agent), bestatine (immunological response modifier) [8]. The solubility of the Mannich derivatives increases in water due to protonation of basic amine nitrogen atom [9].

2. Materials and Methods

Through two steps, first include syntheses of Mannich bases and preparation of stock solution

Preparation of compound (1) (KI 6) [10, 11]

Add to a mixture of indole (0.0129 mol) and 20 ml of glacial acetic acid
(0.0129 mol (0.474ml) of formaldehyde. The mixture is cooled to a temperature of 5 °C, then dimethylamine (0.0.0129 mol) was added to the mixture. The solution was heated under reflux in water bath for 12hr,75-85C0 and stirred at room temperature for 24hr. 10% NaOH was added to the reaction mixture, Recrystallized by methanol gave pure product. TLC was used to check the reaction result and purity of product by using mixture of Ethanol: H2O (1:1). Also column chromatography was used to get ultrapure yield by using same mixture as mobile phase and silica gel (220-240 mesh) as stationary phase yielded 68% crystalline solid m.p.120C0.

doi.org/10.31838/hiv22.02.258 Received: 21.05.22, Revised: 22.06.22, Accepted: 01.08.22

Preparation of compound (21) KI4

5 mmol (0.87 g) of (1) KI6 is dissolved in hot distilled water, then (2 mmol) (0.08 g) of sodium hydroxide dissolved in (10 ml) of hot distilled water is added to it. Mercuric chloride (2.6 mmol) (0.71 g) of dissolved in (10 ml) hot distilled water, to which (10 ml) absolute ethanol is addedto the mixture, and the mixture is reacted in a water bath (60-65) ° C for 2 hours, then filtered, the precipitate is washed with ethanol and crystallized obtained compound (19). Added (40 ml) of toluene to (2.3 mmol)(0.28 g) of (1,3,4,6- tetra-O-benzoyl-β-D-fructofuranose) in the presence of a boiling stone, (2.3 mmol) of (0.1 g) of ((3-dimethylamino)methyl)-1H-indol-1-yl)mercury(II) Chloride)(19) added to the mixture. At (130-1350C) refluxed with stirring the mixture for 3.5hr and then filtrate, washed by CHCl3and crystallized. A residue was obtained as red crystal (0.43g) (27%yield). IR (film), 1456 cm-1 of (C-N) compound (20). (1g, 1.32mmol) from (20) in (45ml) ethanol absolute with (2-3) drops of 36%HCl. The mixture was refluxed with stirring for 1.5 hr
And evaporated to dryness to give a red powder (0.35g, 79%).As shown in the scheme 2

Preparation of (8) KI2 [13, 14]

Add to a mixture of indole (0.0129 mol) and 20 ml of glacial acetic acid
(0.0129 mol (1.314ml) of Benzaldehyde. The mixture is cooled to a temperature of 5 °C, then Dimethylamine (0.0.0129 mol) (0.8664ml) was added to the mixture. The solution was heated under reflux in water bath for 12hr,85-95C0 and stirred at room temperature for 24hr. 10% NaOH was added to the reaction mixture, Recrystallized by ethyleacetate and H2O gave pure product. TLC was used to check the reaction result and purity of product by using mixture of Ethanol: H2Othyleacetate (1:1). Also column chromatography was used to get ultrapure yielded (2.34g) by using same mixture as mobile phase and silica gel (220-240 mesh) as stationary phase. As shown in the scheme 3.

Preparation of (24) KI1

5 mmol (0.87 g) of (8) KI2 is dissolved in hot distilled water, then (2 mmol) (0.08 g) of sodium hydroxide dissolved in (10 ml) of hot distilled water is added to it. Mercuric chloride (2.6 mmol) (0.71 g) of dissolved in (10 ml) hot distilled water, to which (10 ml) absolute ethanol is addedto the mixture, and the mixture is reacted in a water bath (60-65) ° C for 2 hours, then filtered, the precipitate is washed with ethanol and crystallizedobtained compound (23). Added (40 ml) of toluene to (2.3 mmol)(0.28 g) of (1,3,4,6- tetra-O-benzoyl-β-D-fructofuranose) in the presence of a boiling stone, (2.3 mmol) of (0.1 g) of ((3-dimethylamino)phenyl)-1H-indol-1-yl)mercury(II) Chloride)(23) added to the mixture. At (130-1350C) refluxed with stirring the mixture for 3.5hr and then filtrate, washed by CHCl3and crystallized. A residue was obtained as red crystal (0.43g) (27%yield). IR (film), 1456 cm-1 of (C-N) compound (23). (1g, 1.32mmol) from (23) in (45ml) ethanol absolute with (2-3) drops of 36%HCl. The mixture was refluxed with stirring for 1.5 hr
And evaporated to dryness to give a red powder (24) KI1 (0.35g, 79%).

Preparation stock solution of CT-DNA

Stock solution of DNA was prepared by dissolving 10 mg of calf-thymus DNA per milliliter of 10 mM Tris–HCl buffer (pH 7.4). The stock solution was kept at 8 C for 24 h and stirred occasionally for complete homogenization. Final concentration of the stock CT-DNA solution was measured spectrophotometrically using excitation coefficient of 6600 cm-1 [12]. The UV absorbance of 250 time's diluted CT-DNA solution was found 0.740 at 260 nm with a path length of 1 cm. The final concentration of CT-DNA stock solution was 28 mM (molarity of phosphate group) [13].

Preparation stock solution of Idole derivatives [KI1]

The indole derivatives [KI1] solution was prepared in ultra-pure water and incubated for 96 h for complete hydrolysis. A series of solutions with varying concentrations of [KI1] were prepared. [KI1] solutions of different concentration so prepared were added drop wise to CT-DNA solutions.
The [KI1]/CTDNA ratios (r) were kept 1/100, 1/50, 1/20, 1/10 and 1/5. The final concentration of the DNA was 14 mM in all the solutions used for infrared measurement [13].

3. Result and Conclusion

Identification of compound (1) KI6

It's IR (FT-IR Shimadzu Fourier Transform Infrared Spectrophotometer 8400 S (KBr) showed absorption frequencies (in cm^{-1}) in table 1 at 3404 (NH), 2962 (CH) aliphatic, 3053 (CH) aromatic, 1616 (C=C) aromatic, 1456 (C-N). H^1NMR spectrum (Proton Nuclear Magnetic Resonance Spectroscopy – Bruker Ultra shield 400 MHZ – By using (TMS) as reference and (DMSO d6) as solvent) in table 2 (δ, 1.9 ppm, singlet) due to the protons of (CH_3) at position C11, C 12. At (δ, 3.36ppm, singlet) single appeared due to the (CH_2) protons at position C10. The signal that appeared at (δ, 8.20, 7.02. ppm, d) due to tow protons C4, C7. Signal appeared at (δ, 6.66-7.52 ppm, and m) due to tow protons C5, C6.singlet signal appeared at (δ, 7.13 ppm, and s) due to single proton at position C2. At last we found singlet signal at (δ, 10 .74 ppm s) back to NH at N1. As shown in the scheme 2

Table (1): FT-IR absorption values for compounds (KI6,KI4)

Comp. NO.	Structure	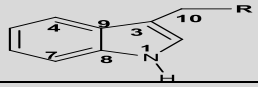					
		IR υ cm-1 (KBr)					
		N-H	C-H Aliph	C-H Ar.	C=C Ar.	C-N	Others

Indole	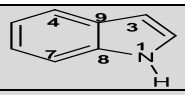	3396	2983	3047	1614	1454	
(1)KI6	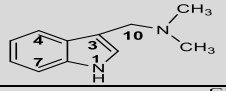	3404	2962	3053	1616.	1456	
(21)KI4	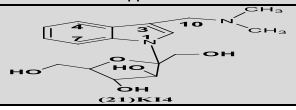	-----	2866	2906	1600	1456	3373 OH

Table (2): 1H-NMR values for compound (1) KI6,

Comp. No	Structure	Chemical Shift ppm	Type of signal	Position of H
(1) KI 6	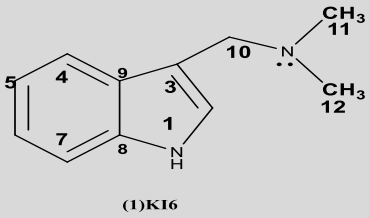 (1)KI6	2.5 CH3	S	DMSO
		1.92 CH3	S	C11,C12
		3.36 CH2	S	C10
		7.13 CH	S	C2
		8.20 CH	d	C4
		7.02 CH	d	C7
		7.31 CH	m	C5
		7.52 CH	m	C6
		10.74 NH	S	N1
S = singlet , d=doublet , t= triplet , m= multiplet				

Table (3): 1H-NMR values for compound (21) KI4

Comp. No	Structure	Chemical Shift ppm	Type of signal	Position of H
(21)KI4	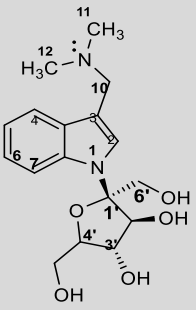 (21) KI 4	2.5 6H CH3	S	DMSO
		2.06 6H CH3	S	C11,C12
		3.39 2H CH2	S	C10
		8.1 1H CH	S	C2
		4.71 (4 OH)	S	C6',C2',C3',C5'
		3.72 5H CH, CH2	t	C2',C5',C6'
		3.42 2H CH	m	C3',C4'
		8.20 1H CH 7.441H CH	d d	C4 C7
		7.10 1H CH 7.35 1H CH	t t	C5 C6
		11.02	S	H-bond
s = singlet , d=doublet , t= triplet , m= multiplet				

Identification of compound (21) KI4

IR (KBr disc), 3370cm-1brod of (OH) obtained compound (21) KI4 As shown in the scheme 2 table1. The spectrum IR for compound (21)KI4 appeared bands absorption at(3373.61 Cm-1)ben for OH and disappeared the bands absorption at (3400Cm-1) for NH, bands shifted from (3053Cm-1) to (2906Cm-1) back to CH aromatic, bands shifted from (2962Cm-1) to (2866Cm-1)for CH aliphatic , the spectrum showed bands at (1456Cm-1) for C-N, and bands shifted from (1616.40Cm-1) to (1600Cm-1) .The spectrum H1NMR for compound (21)KI4 appeared singlet signal at (δ, 2.06ppm) six protons for tow methyl group at position C11, C12,singlet signal at (δ, 3.39ppm) for CH2 at C10, singlet signal (δ,8.1ppm) for one proton at C2, appeared singlet signal at (δ,4.71ppm) back to four hydroxyl group C6',C2', C3',C5',the spectrum appeared triplet signal at (δ, 3.72ppm) for five protons C2',C5',C6',multiplet signal at(δ,3.42ppm)for tow protons at position C3',C4', tow doublet signal appeared at (δ,8.20ppm) and (δ,7.44ppm) for tow protons at position C4,C7 respectively, tow triplet signal appeared at (δ,7.10 ppm)and (δ, 7.35ppm) for two protons C5,C6, singlet signal appeared at (δ, 11.02ppm) for hydrogen bond. As shown in the scheme 2 table3

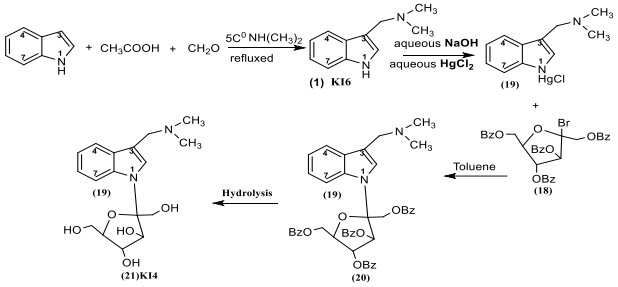

Scheme 2 preparation of compounds (1) KI6 and (21) KI4

Identification of compound (8) KI2

As shown in the scheme 3 table 4. From spectrum IR (8) KI2 we found (N-H)ben peaks appeared of indole in (3417.89 cm-1) , bands absorption at (3055.35 cm-1) appeared back to (C-H)str aromatic, (2920.32cm-1) for (C-H)str aliphatic, bands absorption appearance for (C-N) at (1456.30cm-1) and at (1618.33Cm-1) for (C=C) aromatic. In table 5 The spectrum H1NMR for compound(8) KI2 appeared signal at (δ, 2.51ppm, singlet) due to protons of the solvent (DMSO),singlet signal at (δ,2.09ppm) for two methyl group in position C17,C18,the spectrum appeared tow singlet signals at (δ,5.83ppm), (δ,7.04ppm) for tertiary carbon in C10 and C2, triplet signal appeared at

(δ,7.25-7.29ppm) back to C5,C6 and C13,C14,C15, doublet signal appeared at δ,7.34-7.36ppm) back to C4,C7.The spectrum showed doublet signal too at (δ,6.83-6.86ppm) back to 2H in C12,C16, singlet signal appeared at (δ,10.83ppm) for NH back to N1position. All the values we are corresponding to literatures.

Table (4) shows the FT-IR values for synthesized derivatives (8)KI2,(24) KI1

Comp. NO.	Structure	IR υ cm-1 (KBr)					
		N-H	C-H Aliph	C-H Ar.	C=C Ar.	C-N	Others
(8)KI2	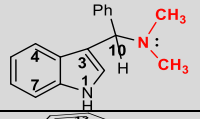	3417	2920	3055	1618	1456	
(24)KI1	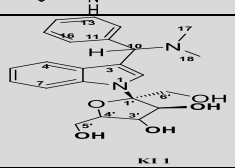	-----	2866	2902	1647	1456	3371 OH

Identification of compound (24) KI1

The spectrum IR for compound (24)KI1 in the table 4 showed bands absorption at(3371.66 Cm-1)ben for OH and disappeared the bands absorption at (3400Cm-1) for NH, bands shifted from (3053Cm-1) to (2902.96Cm-1) back to CH aromatic, bands shifted from (2962Cm-1) to (2866Cm-1)for CH aliphatic , the spectrum showed bands at (1456Cm-1) for C-N, and bands shifted from (1616.40Cm-1) to (1647Cm-1)back to C=C aromatic. By observing the infrared spectrum of the compound (23) which represents the same compound above, except that the hydroxyl groups in the sugar molecule are protected by the benzoyl group, the appearance of bands when absorbing (1753.35 cm-1) belong to the carbonyl groups. The spectrum H1NMR for compound (24) KI1 showed singlet signal at(δ,2.5ppm) due to six protons of the solvent (DMSO),tow singlet signal at (δ, 2.09ppm) back to tow CH3 group in C17,C18, appeared singlet single at(δ, 5.69ppm) for CH in C10, appeared tow doublet single at (δ, 3.43ppm) for CH2 in C6',CH in C2' and OH in C2',C3', appeared triplet signal at (δ,3.71ppm) for CH2, in C5' and OH in C6',the spectrum showed mutiplet signal at (δ,4.71ppm) back to CH in position C3',C4', appeared singlet signal at (δ,8.32ppm) for CH in C2, tow doublet signal appeared at (δ,7.27ppm), (δ,7.32ppm) for CH in C4,C12 and C7,C16 respectively, multeplet signal appeared at (δ, 6.79ppm),C5,C13 (δ,6.96ppm) C6,C14 and (δ, 7.08ppm) C15,the spectrum showed two singlet signal at (δ,10.79 ppm) and (δ,11.03 ppm) back to hydrogen bonds. As shown in the scheme 3 table 6 all the values we are corresponding to literatures.

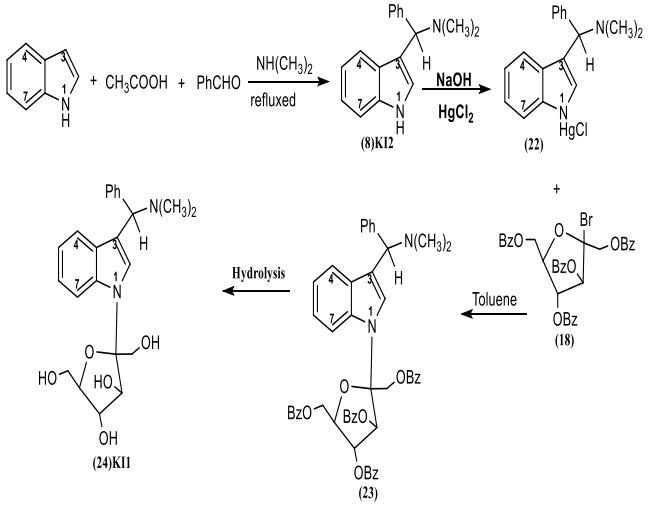

Scheme 3 preparation of compounds (8) KI2 and (24) KI1

Table (5): 1H-NMR values for compound (8)KI2

Comp. No	Structure	Chemical Shift ppm	Type of signal	Position of H
(8) KI 2	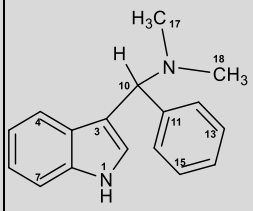	2.5 CH3	S	DMSO
		2.09 CH3	S	C17,C18
		5.7 CH	S	C10
		6.83-6.86 CH	d	C12,C16
		7.92-7.93 CH	d	C4,C7
		7.25-7.29 CH	t	C13,C14,C15
		7.34-7.36 CH	m	C5,C6
		10.83 NH	S	N1
S = singlet , d=doublet , t= triplet , m= multiple				

Table (6) H1NMR Compound (24) KI1

Comp. No	Structure	Chemical Shift ppm	Type of signal	Position of H
(24)KI1		2.5 CH3	S	DMSO
		2.09 CH3	S	C17, C18
		5.69 CH	S	C10
		8.32 CH	S	C2
		7.27 CH	d	C4, C12
		7.32 CH	d	C7, C16
		6.79 CH	m	C5, C13
		6.96 CH	m	C6, C14
		7.08 CH	m	C15

	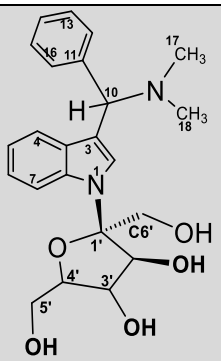 KI 1	3.43 CH2	d	C6'
		3.43 CH	d	C2'
		3.43 OH	d	C2', C3'
		3.72 OH	t	C6'
		3.72 CH2	t	C5'
		4.71 CH	m	C3', C4'
		10.79 H-bond	S	
		11.03 H-bond	S	
S = singlet , d=doublet , t= triplet , m= multiplet ,				

Table 7 physical properties for Indole derivatives.

Comp. NO	Color	m.p C0	%yield
(1)KI6	Red Light orange	120	68
(21)KI4	Red brown	122	76
(8)KI2	Orange	116	73
(24)KI1	brown	128	80

4. Binding with CT-DNA

FT-IR spectra of [KI1]/CT-DNA complex

Base binding

In the [KI1]/CT-DNA complexes (r = 1/100-1/5), the intensity of Gua, Thy, Ade, and Cyt bands slightly changed r = 1/5 for Ade, and at r = 1/10 for Thy, Cyt and Gua (figure (1). As for (R = 1/20, 1/50) for adenine, cytosine observed a slight increase the intensity and a decrease in the density for guanine and adenine. The observed intensity changes can be related to [KI1] interaction with Gua–Cyt and Ade–Thy base pairs. At r = 1/5, shifting for the bands at 1649 (Gua) to 1645, at 1631 (Thy) to 1629, 1519 (Ade) to 1516, and phosphate bands at 1197 t0 1383. As for cytosine, it doesn't shifted.

The observed shifting was accompanied by a decrease in the intensity of the DNA bases except for the Ade, Cyt which could be ascribed to a certain degree of helix instability [13] As [KI1] concentration increased (r = 1/20-10), shifting for the bands at 1631 (Thy) to 1629, 1519 (Ade) to 1518, 1467 (Cyt) does not shift and phosphate bands at 1197 shifted to1319 (figures (1) was observed in the spectra of [KI1]–DNA complexes. In addition, a major increase in the intensities of Ade was observed, indicating a major interaction with Ade–Thy base pairs (minor groove). This should also be due to the fact that Ade and Thy bases interact through two hydrogen bonds while Cyt and Gua bases are stabilized by three hydrogen bonds, which account for the former being more prone to perturbation and interaction by [KI1], offering steric advantages for the molecular interaction. Indeed, some ligand prefers Ade–Thy regions of B-DNA for binding because of the narrower minor groove in Ade–Thy regions (as compared to Gua–Cyt regions of B-DNA) leads to a snug fit of the flat aromatic [KI1] rings between the walls of the groove; also, the higher negative electrostatic potential, attributable in part to the absence of electropositive ANH2 groups along the floor of the groove and the steric advantage of the absence of those same Gua ANH2 groups permit the drug molecule to sink deeper into the grove [14]. In addition, these experiments demonstrated that [KI1] is a good electron acceptor with high polarization ability and dipole moment values, while Ade–Thy and Gua–Cyt base pairs are good electron donors, which are favorable for the aromatic stacking interactions between these two systems [15]. Minor increase in the intensities of Cyt, VsPO2 (symmetrical stretching) at ratios r = 1/100-20 are also indicative of some degree of [KI1] interactions with Gua–Cyt base pairs and phosphate groups. This could be explained by some hydrophobic interaction via of ligand with Cyt [16]. At r = 1/10, some reduction in the intensity ratios of the bands at 1647 (Gua), 1626 (Thy), (Ade) does not shifted, 1464 (Cyt), and 1384 (VsPO2) were observed (figure (1). These losses of intensity ratios were probably due to aggregation of DNA complexes [17]. The major spectral shifting observed for [KI1] in-plane vibrations, are also characteristic of [KI1] interaction via anion- specific donor site. [KI1] is in monovalent anion form Wang et al. [18] the infrared bands at 3371, 1647, 2902, cm-1, assigned to the free [KI1] in-plane OH, C=C, -CH-aromatic, stretching vibrations [19], exhibited major shifting upon CT-DNA complexation (figure (1). r = 1/10). The observed spectral changes point to a major [KI1]/CT-DNA interaction through the [KI1] C=O group. Similar behavior was observed in the infrared spectra of the aspirin–DNA and ascorbate–DNA complexes [20].

Phosphate binding

The phosphate asymmetric stretching at 1197 cm-1 and symmetric stretching at 1093 cm-1 in the spectrum of free DNA is shifted to 1383 and 1045 cm-1, respectively, when lower concentration of [KI1] is complexed with DNA (r = 1/5; figure (5). Further shifting toward lower wave number (1383 cm-1 for asymmetric PO2 stretching and 1045 cm-1 for symmetric PO2 stretching) is observed when [KI1] is complexed with DNA at higher concentration (r < 1/100) figure (1)

These results also suggest some weak external interaction of [KI1] with the phosphate backbone upon its interaction with the DNA double helix and corroborate with observations by Bi and co-workers [21] who in FT-IR studies on DNA–[KI1] interaction observed a shift at 1241– 1263 cm-1 (asymmetric PO2 stretch) but, due to non-satisfactory resolution, could not determine the specific interacting bases.

CT-DNA conformation

Free CT-DNA show B conformation with infrared marker

bands at 1649 cm-1 (Gua), 1197 cm-1 (asymmetric PO2 stretch), 670cm-1 (sugar-phosphate stretch), and 607 cm-1 (phosphodiester mode). In a B-to-A transition, B DNA marker bands at 844 cm-1 due to phosphodiester mode and at 1645 cm-1 due to Gua shift toward lower frequencies, in addition, the band at 1197 cm-1 due to symmetric phosphate vibrations shifts towards higher frequencies about 1315–1383 cm-1 [22, 23]. When a B to Z transition takes place, the band at 607 cm-1 displaces to ca. 844 cm-1 and the band at 1647 cm-1 appears near 1645 cm-1, whereas the band at 1197 cm-1 shifts toward 1383 cm-1 [17]. The changes observed in the bands at 1645 cm-1 and 1197 cm-1 are not indicative of CT-DNA conformational change. The minor spectral change observed in the deoxyribose region 900–500 cm-1 may be attributed to minor alterations in the sugar-phosphate geometry while DNA remains in B state of conformation.

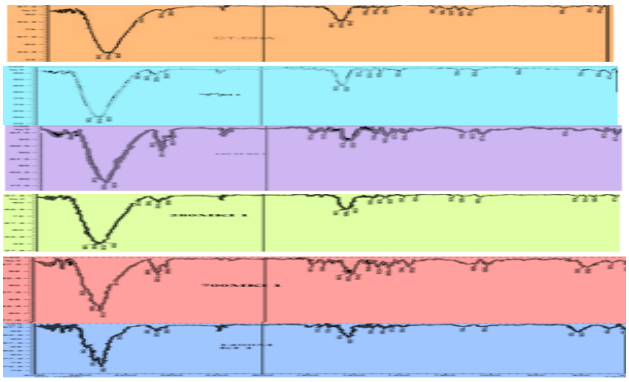

Figure (1) IR spectra of [KI1]/CT-DNA complex

UV-Visible

UV spectra of calf-thymus DNA with varying concentrations of [KI1]. There are four major bands in the spectra for pure DNA, 215 nm (negative), 206 nm (positive), 235 nm (negative), 255 nm (negative) and 265 nm (positive). These are marker UV bands of double helical DNA in B-conformation [15-24]. When B-to-A DNA transition occurs, UV band at 215 nm becomes less intense, band at 206 nm shifts toward higher wavelength, and band at 265 nm becomes more intense Subastri [25]. Binding of [KI1] with CT-DNA does not cause any appreciable shifting in these marker UV bands, indicative of no alteration in B-DNA conformation. This is further confirmed with our infrared spectroscopic results of [KI1]–DNA interactions, which shows no changes for B-DNA marker bands at 1197 cm-1 (PO2) and 607 cm-1 (phosphodiester modes). It should be noted that in a B-to-A transition, these B-DNA marker bands shift from 1197 to 1383 cm-1 (PO2) and 607 to 844 cm-1 (phosphodiester) [26-30]. We decided these spectral shifting in IR spectra.

The reduction in the intensity of band In the UV spectra at 264 nm is observed for high [KI1] concentrations (r = 1/10 and 1/5). This change may be attributed to CT-DNA aggregation as [KI1] content increases in CT-DNA/drug complexes [28, 31, 32].

The graph in figure (2) for the UV rays of the free and complex DNA, where the binding constant K is calculated by calculating the cross-slope ratio.

Table (8) UV-Visible Absorbance values of the compound (KI 1) at different concentrations					
1/C KI 1	**2.94**	**5.88**	**12.5**	**27.7**	**58.8**
1/ A-A0	43.4	7.8	62.5	24.4	3.93

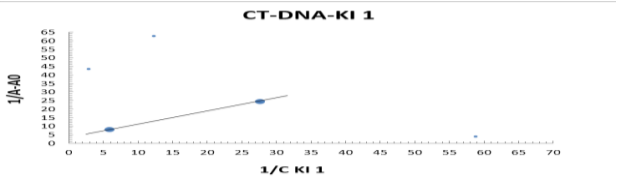

Figure (2) UV-Visible CT-DNABinding with compound KI 1

K = 0.76 = Binding conistand

A0 = the initial absorbance of free DNA nucleic acid

A = the absorbance with different concentration of KI1 at 260 nm

CKI 1 = concentration of compound KI1 in solution

Bioactive for compounds KI1

Where it was distinguished that the compound (KI1) has an inhibition zone against positive bacteria is higher than the inhibition zone against fungi (Candidate albicans). While there is no inhibition against gram-negative bacteria (S. aureus) this we can see clearly through the table (9) and figure (3).

Table (9) inhibition zone for compound KI1			
KI1	**E.coil**	**S. aureus**	**Candidate albicans**
Cont.	0	0	0
100%	0	29	20

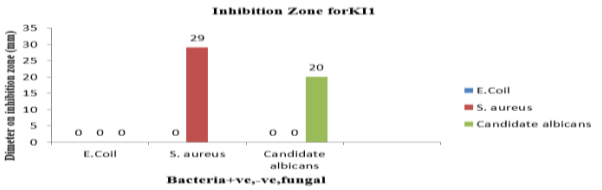

Figure (3) Bioactive compound KI 1against bacteria +ve,-ve and fungal

References

1. Tramontini M. Advances in the chemistry of Mannich bases. Synthesis. 1973;1973(12):703-75. https://doi.org/10.1055/s-1973-22294

2. Tramontini M, Angiolini L. Further advances in the chemistry of Mannich bases. Tetrahedron. 1990;46(6):1791-837. https://doi.org/10.1016/S0040-4020(01)89752-0

3. Nie J, Guo H-C, Cahard D, Ma J-A. Asymmetric construction of stereogenic carbon centers featuring a trifluoromethyl group from prochiral trifluoromethylated substrates. Chemical Reviews. 2011;111(2):455-529. https://doi.org/10.1021/cr100166a

4. Kang YK, Kim DY. Catalytic asymmetric Mannich-type reactions of fluorinated ketoesters with N-Boc aldimines in the presence of chiral palladium complexes. Tetrahedron Letters. 2011;52(18):2356-8. https://doi.org/10.1016/j.tetlet.2011.02.087

5. Yang Y, Phillips DP, Pan S. A stereoselective approach to 6-alkylated piperidinone & 2-piperidine via three-component vinylogous Mannich reactions (VMR) and a concise synthesis of (S)-anabasine. Tetrahedron letters. 2011;52(14):1549-52. https://doi.org/10.1016/j.tetlet.2011.01.090

6. Martin SF. Evolution of the vinylogous Mannich reaction as a key construction for alkaloid synthesis. Accounts of chemical research. 2002;35(10):895-904. https://doi.org/10.1021/ar950230w

7. Liu M, Sibi MP. Recent advances in the stereoselective synthesis of β-amino acids. Tetrahedron. 2002;40(58):7991-8035.

8. Sarhan AEWA, Abdel-Hafez SH, El-Sherief H, Aboel-Fadl T. Utility and Synthetic Uses of Mannich Reaction: An Efficient Route for Synthesis of Thiadiazino-[1, 3, 5][3, 2-a] benzimidazoles. Synthetic communications. 2006;36(8):987-96. https://doi.org/10.1080/00397910500501243

9. Sumalatha Y, Reddy PP, Reddy R, Satyanarayana B. Synthesis and spectral characterization of process-related substances to the hypnotic agent zolpidem. Arkivoc. 2009;7:143-9.

10. Al-Araji SM, Ali RA. Synthesis of new Mannich bases from indole derivatives. Baghdad Science Journal. 2012;9(1).

11. Ali NAW, Al-Lami SH. Oral Hygiene Status and Gingival Health of Children at Age 4-12 Years in Baghdad. Journal of the College of Dentistry. 2003;1:27.

12. Vijayalakshmi R, Kanthimathi M, Subramanian V, Nair BU. DNA cleavage by a chromium (III) complex. Biochemical and biophysical research communications. 2000;271(3):731-4. https://doi.org/10.1006/bbrc.2000.2707

13. Saito ST, Silva G, Pungartnik C, Brendel M. Study of DNA–emodin interaction by FTIR and UV–vis spectroscopy. Journal of Photochemistry and Photobiology B: Biology. 2012;111:59-63. https://doi.org/10.1016/j.jphotobiol.2012.03.012

14. Reddy BP, Sondhi SM, Lown JW. Synthetic DNA minor groove-binding drugs. Pharmacology & therapeutics. 1999;84(1):1-111. https://doi.org/10.1016/S0163-7258(99)00021-2

15. Riahi S, Eynollahi S, Ganjali MR. Interaction of emodin with DNA bases: a density functional theory. Journal of Theoretical and Computational Chemistry. 2010;9(05):875-88. https://doi.org/10.1142/S0219633610006055

16. Biological ISf, Repositories E. Collection, storage, retrieval and distribution of biological materials for research. Cell Preservation Technology. 2008;6(1):3-58. Available from: https://www.liebertpub.com/na101/home/literatum/publisher/mal/journals/content/cpt/2008/cpt.2008.6.issue-1/cpt.2008.9997/production/cpt.2008.9997.fp.png_v03

17. Jangir DK, Tyagi G, Mehrotra R, Kundu S. Carboplatin interaction with calf-thymus DNA: A FTIR spectroscopic approach. Journal of Molecular Structure. 2010;969(1-3):126-9. https://doi.org/10.1016/j.molstruc.2010.01.052

18. Wang D, Yang G, Song X. Determination of pKa values of anthraquinone compounds by capillary electrophoresis. Electrophoresis. 2001;22(3):464-9. https://doi.org/10.1002/1522-2683(200102)22:3%3C464::AID-ELPS464%3E3.0.CO;2-4

19. Harry-O'kuru RE, Wu YV, Evangelista R, Vaughn SF, Rayford W, Wilson RF. Sicklepod (Senna obtusifolia) seed processing and potential utilization. Journal of agricultural and food chemistry. 2005;53(12):4784-7. https://doi.org/10.1021/jf040483g

20. Arshad N, Zafran M, Ashraf Z, Perveen F. Synthesis, characterization of amide substituted dexibuprofen derivatives and their spectral, voltammetric and docking investigations for DNA binding interactions. Journal of Photochemistry and Photobiology B: Biology. 2017;169:134-47. https://doi.org/10.1016/j.jphotobiol.2017.02.021

21. Bi S, Zhang H, Qiao C, Sun Y, Liu C. Studies of interaction of emodin and DNA in the presence of ethidium bromide by spectroscopic method. Spectrochimica Acta Part A: Molecular and Biomolecular Spectroscopy. 2008;69(1):123-9. https://doi.org/10.1016/j.saa.2007.03.017

22. Nafisi S, Norouzi Z. A comparative study on the interaction of cis-and trans-platin with DNA and RNA. DNA and Cell Biology. 2009;28(9):469-77. https://doi.org/10.1089/dna.2009.0894

23. Nafisi S, Kahangi FG, Azizi E, Zebarjad N, Tajmir-Riahi H-A. Interaction of zanamivir with DNA and RNA: Models for drug–DNA and drug–RNA bindings. Journal of molecular structure. 2007;830(1-3):182-7. https://doi.org/10.1016/j.molstruc.2006.09.032

24. Vorlíčková M, Kejnovská I, Bednářová K, Renčiuk D, Kypr J. Circular dichroism spectroscopy of DNA: from duplexes to quadruplexes. Chirality. 2012;24(9):691-8. https://doi.org/10.1002/chir.22064

25. Subastri A, Ramamurthy C, Suyavaran A, Rao PL, Babu EP, Krishna KH, Kumar MS, Thirunavukkarasu C. Probing the interaction of troxerutin with transfer RNA by spectroscopic and molecular modeling. Journal of Photochemistry and Photobiology B: Biology. 2015;153:137-44. https://doi.org/10.1016/j.jphotobiol.2015.09.013

26. Agudelo D, Kreplak L, Tajmir-Riahi H. Microscopic and spectroscopic analysis of chitosan–DNA conjugates. Carbohydrate polymers. 2016;137:207-13. https://doi.org/10.1016/j.carbpol.2015.09.080

27. CN N. soukpoe-Kossi, AA Ouameur, T. Thomas, A. Shirahata, TJ Thomas and HA Tajmir-Riahi. Biomacromolecules. 2008;9:2712-8.

28. Abderrezak A, Bourassa P, Mandeville J-S, Sedaghat-Herati R, Tajmir-Riahi H-A. Dendrimers bind antioxidant polyphenols and cisplatin drug. PloS one. 2012;7(3):e33102. https://doi.org/10.1371/journal.pone.0033102

29. Al-doury S, Al-Nasrawi M, AL-Samarraie M. The molecular sequence of Giardia lamblia by using (tpiA) and (tpiB). International Journal of Drug Delivery Technology. 2019;9(03):374-7.

30. Mustafa M, AL-Samarraie M, Ahmed M. Molecular techniques of viral diagnosis, Science Archives, 1 (3), 89-92http. dx doi org/1047587/SA. 2020.

31. AL-Samarraie MQ, Omar MK, Yaseen AH, Mahmood MI. The wide spread of the gene haeomolysin (Hly) and the adhesion factor (Sfa) in the E. coli isolated from UTI. Journal of Pharmaceutical Sciences and Research. 2019;11(4):1298-303.

32. Al-samarraie mq, yaseen[1] ah, ibrahim bm. Molecular study of polymorphism for gene tnf-alpha using arms-pcr technique for patients with rheumatoid arthritis. Biochem cell arch vol. 2019;19:4285-90.